Entropy driven phase transition in itinerant antiferromagnetic monolayers

R. Wieser, E. Y. Vedmedenko, and R. Wiesendanger
Institut für Angewandte Physik und Zentrum für Mikrostrukturforschung, Universität Hamburg, Jungiusstrasse 11, D-20355 Hamburg, Germany

(Received 13 August 2007; revised manuscript received 10 December 2007; published 8 February 2008)

Based on Monte Carlo calculations, the magnetic ordering in itinerant antiferromagnetic monolayers with geometric frustration has been analyzed. For description of the itinerant magnetism exchange interactions beyond the Heisenberg model such as the biquadratic exchange and the four-spin exchange interaction have been taken into account. We demonstrate that the higher-order exchange interactions remove the structural degeneracy and lead to configurational phase transitions at finite temperatures. A new, entropy driven structural phase transition in V/Ag(111) is predicted theoretically.

DOI: 10.1103/PhysRevB.77.064410 PACS number(s): 75.70.Ak, 75.10.Hk, 65.40.G−, 75.40.Mg

I. INTRODUCTION

Substantial part of contemporary experimental studies on magnetic nanostructures is concerned with transition 3*d* and 4*d* metals or their alloys on different substrates. Magnetic properties of these systems are dominated by the itinerant nature of delocalized *d* electrons. Theoretically, magnetic ordering in itinerant systems can be accurately described in the framework of density functional theories (DFTs).[1–5] DFT calculations provide a full description of a charge- and spin-density distributions of a system on which base one can derive the strength of magnetic anisotropy, exchange interactions, and atomic magnetic moments. However, the *ab initio* methods are able to address only rather small systems (tens of atoms) while even a very small $2\times2\times2$ nm^3 Co nanostructure contains about 1000 atoms. Because of this limitation, only ideal magnetic configurations with a small unit cell can be treated within these approaches, more complicated domain or superstructures cannot be addressed. Usually, for DFT calculations, a particular magnetic configuration has to be assumed; i.e., stochastic optimization of a configuration is unavailable. This limits the possibility of interpretation of magnetic frustration, which may lead to unexpected hierarchic interpenetrating magnetic structures.[6] Another limitation is the incorporation of the temperature and weaker long-range many-body interactions such as magnetic dipolar coupling into the treatment because of the huge computer power demands. Therefore, the data on the thermodynamic properties of itinerant nanomagnets as well as the magnetic ordering due to the delocalized electrons are very limited so far.

Another possibility to take the itinerant nature of 3*d* magnets into account is the extension of the classical exchange Hamiltonian by terms beyond the nearest-neighbor Heisenberg coupling. These terms can be derived by means of the fourth order perturbation expansion of the Hubbard model[7] as the third order treatment leads to zero terms in the absence of spin-orbit interaction.[8] Apart of the effective, longer-range Heisenberg-like terms, the most important higher-order contributions are the biquadratic and the four-spin exchange interaction resulting from the hopping of electrons over four neighboring sites. Although the mathematical form of those terms is well known,[9] a general study of the magnetic structuring in the itinerant magnets is still lacking.

The aim of this investigation is a systematic description of the magnetic ordering in itinerant systems. Toward this end, we incorporate the higher-order exchange contributions into the classical Monte Carlo scheme and explore the phase space for pure biquadratic and four-spin exchange interactions. Then, we study the magnetic ordering and the thermodynamic properties of Mn and V monolayers on Cu(111) and Ag(111), respectively, and compare our results with recent first-principles calculations.[9,10]

The publication is organized as follows. In Sec. II, the model and the Monte Carlo procedure are described. Section III is devoted to the general analysis of higher-order interactions. In Sec. IV, we explore ground states of Mn/Cu(111) and V/Ag(111), while the thermodynamic behavior of those systems is described in Sec. V.

II. MODEL

We consider a classical spin model, which is described by the following Hamiltonian:

$$\begin{aligned}\mathcal{H} = &\sum_{i<j} J_{ij}\mathbf{S}_i\cdot\mathbf{S}_j + J_{bi}\sum_{\langle ij\rangle}(\mathbf{S}_i\cdot\mathbf{S}_j)^2 \\ &+ D_z\sum_i (S_{zi})^2 - \omega\sum_{i<j}\frac{3(\mathbf{S}_i\cdot\mathbf{e}_{ij})(\mathbf{e}_{ij}\cdot\mathbf{S}_j)-\mathbf{S}_i\cdot\mathbf{S}_j}{r_{ij}^3} \\ &+ J_{4\text{-}spin}\sum_{\langle ijkl\rangle}[(\mathbf{S}_i\cdot\mathbf{S}_j)(\mathbf{S}_k\cdot\mathbf{S}_l) \\ &+ (\mathbf{S}_i\cdot\mathbf{S}_k)(\mathbf{S}_j\cdot\mathbf{S}_l) - (\mathbf{S}_i\cdot\mathbf{S}_l)(\mathbf{S}_j\cdot\mathbf{S}_k)] \qquad (1)\end{aligned}$$

where the $\mathbf{S}_i=\boldsymbol{\mu}_i/\mu_s$ are three dimensional magnetic moments of unit length on a triangular lattice with open boundaries; μ_s is the absolute value of the magnetic moment which is of the order of a few Bohr magneton μ_B.

The first sum describes the exchange interactions of the Heisenberg form up to third nearest neighbor. $J_{ij}<0$ means a ferromagnetic and $J_{ij}>0$ an antiferromagnetic exchange coupling. The second term is the biquadratic exchange between two nearest-neighboring spins. The third sum describes a uniaxial anisotropy favoring a vertical (z) orientation of magnetization for negative, while an in-plane (xy) alignment of magnetic moments for positive anisotropy con-

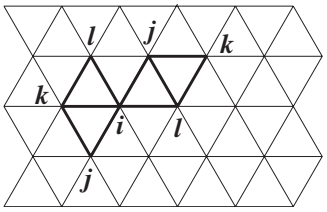

FIG. 1. Minimal parallelograms of the four-spin interaction on the triangular lattice.

stant D_z. The fourth sum is the long-range dipolar interaction with the coupling constant $\omega=\mu_s^2\mu_0/4\pi a^3$. The distances between moments i and j normalized to the lattice spacing a are denoted as r_{ij}, while the unit vectors pointing from spin i to j as $\mathbf{e}_{ij}$. The long-range dipolar interaction has been calculated with the help of a fast Fourier transformation technique to decrease the numerical effort.[11,12] The last part of the Hamiltonian is the four-spin interaction. We restrict ourselves to the nearest-neighbor couplings only. In the case of a triangular lattice, the four involved sites i, j, k, and l form a minimal parallelogram, where each side is a line connecting two nearest neighbors (see Fig. 1). In total, there exist 12 minimal parallelograms for each central magnetic moment i. Two examples of minimal parallelograms are shown in Fig. 1.

All the parameters used in the Hamiltonian above are expressed as energies per atom.

In simulations, a heat-bath Monte Carlo method discussed in Refs. 13–15 has been used. The method is based on a single spin flip algorithm. The trial step consists of a random movement of a magnetic moment $\mathbf{S}_i$ within a certain maximum solid angle depending on the temperature.[15] The energy of new configuration $\mathcal{H}(\mathbf{S}_i')$ is computed according to Eq. (1). Finally, the new configuration is accepted with the heat-bath probability,

$$w_{\mathbf{S}_i\to\mathbf{S}_i'}=\frac{w_0}{1+\exp\left(\dfrac{\mathcal{H}(\mathbf{S}_i')-\mathcal{H}(\mathbf{S}_i)}{kT}\right)}, \tag{2}$$

for an arbitrary constant w_0. Scanning the lattice and performing the procedure explained above once per spin, on average, compose one Monte Carlo step (MCS).

To study the thermodynamical properties and the ground magnetic states of itinerant systems, a slow annealing procedure has been applied. The cooling down with at least 100 temperature steps each consisting of 10 000 MCS has been performed. All thermodynamic characteristics have been calculated in the framework of the fluctuation-dissipation theorem by complete time and sample averaging. The finite size scaling has been performed for lattices from 16×16 until 256×256 magnetic moments. In the following, the central portions of the largest sample are shown.

III. GROUND STATES FOR THE PURE BIQUADRATIC AND FOUR-SPIN EXCHANGE INTERACTIONS

In order to understand the action of the Hamiltonian in its all variety, one should first comprehend the requirements of individual contributions. Whereas ground states of systems coupled via longer-range Heisenberg exchange interactions have been recently investigated,[9,10] the spin structure of ultrathin films due to the biquadratic and the four-spin interactions has mainly remained concealed. In the following, we explore the ground states of the two higher-order couplings for positive and negative interaction constants on a triangular lattice.

Similar to the direct exchange, the biquadratic and the four-spin contributions depend only on the mutual angle between neighboring magnetic moments θ. Therefore, in the following, we characterize the configurational space by the value of θ:

$$\theta=\arccos(\mathbf{S}_1\cdot\mathbf{S}_2). \tag{3}$$

For collinear states, θ is equal to 0° or 180°. All intermediate θ values belong to the noncollinear configurations. First, we discuss the energy space of simple, two- and four-spin plaquettes for pure biquadratic and four-spin interactions, respectively. Then, we generalize our reasoning for infinite lattices.

The energy extrema (maxima and minima) of the biquadratic exchange [second term in Eq. (1)] are given by $\theta=0°$, 180° or $\theta=90°$, depending on the sign of the interaction constant. For positive coupling ($J_{bi}>0$), a noncollinear 90° configuration of zero energy is the ground state, while the collinear states possess the highest energy. In the case of negative J_{bi}, the ground state is degenerated: the parallel as well as the antiparallel orientation of neighboring magnetic moments have identical energy $E_{bi}=J_{bi}$, whereas the noncollinear 90° state is completely unfavorable. The above argumentation is visualized in a phase diagram, Fig. 2(a). The minimal energies are shown as solid, while the maxima as dashed lines. All the other possible states lie in-between the depicted borders.

For the four-spin, nonlocal exchange [the last term in Eq. (1)], the same consideration can be done with the difference that the interaction of four neighboring spins must be analyzed at the same time. Here, again, the minimal and maximal energies correspond to the collinear magnetic configurations; i.e., cos θ between each pair of spins is ±1 and the energy per plaquette is given by $\mathcal{H}_{4-spin}=\pm J_{4-spin}$. The phase diagram of a plaquette coupled by the four-spin interaction only is shown in Fig. 2(b). For the positive coupling ($J_{4-spin}>0$), a ground state configuration ($E_{4-spin}=-J_{4-spin}$) consists of three parallel and one antiparallel aligned magnetic moments. In the case of negative J_{4-spin}, two different collinear states possess the minimal energy $E_{4-spin}=-J_{4-spin}$. One of them is just a parallel alignment of all four magnetic moments, while another one consists of two pairs of parallel spins which are mutually oriented in opposite directions [see insets of Fig. 2(b)].

With this information, ground states of an infinite system on a triangular lattice coupled by the pure biquadratic or pure four-spin interaction can be constructed and checked by means of Monte Carlo simulations. The simulated ground states for $J_{bi}>0$ and $J_{4-spin}>0$ are given in Fig. 3. As can be seen from the inset, the ground state of a biquadratic system with positive coupling constant is just an orthogonal orienta-

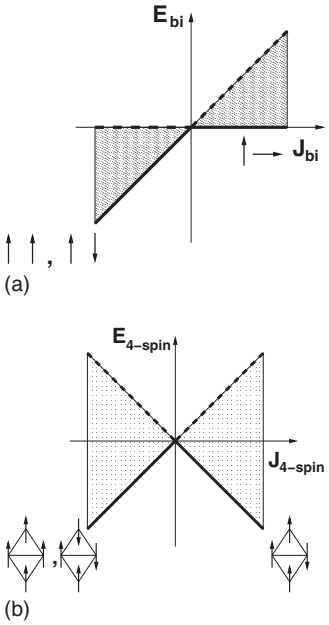

FIG. 2. Phase diagram of a spin system coupled by a pure biquadratic exchange interaction (a) and a four-spin exchange interaction (b) only. The solid lines mark the ground state energies, and the dashed lines correspond to the highest possible energy states. The hatched areas denote all available energy values while the pictograms exemplify states of lowest energy.

tion of nearest-neighboring moments. On a triangular lattice consisting of N sites, there exist $W_{+}^{bi}=3!\cdot 2^{N}$ possibilities to have all neighbors orthogonal up to the global rotation of the spins. For $J_{bi}<0$, the ground state is as expected a collinear configuration. The number of available states in this case is $W_{-}^{bi}=2^{N}$ because of the degeneracy of parallel and antiparallel orientation of neighboring moments. Similar to an Ising antiferromagnet on a triangular lattice,[16,17] the number of ground state configurations in both cases increases drastically with the size of a lattice. Therefore, the systems coupled by a biquadratic exchange interaction possess a residual entropy of $S_{N\to\infty}^{bi}\approx \ln 2$.

In the case of pure J_{4-spin}-coupling, the spin structure has to be constructed with the help of the four-spin plaquettes [see inset of Fig. 2(b)]. If the coupling constant is negative ($J_{4-spin}<0$), there are four possible plaquette configurations, one with just a parallel alignment of all four magnetic moments and three with two pairs of parallel spins which are antiparallel oriented in opposite directions. This degeneracy leads to either a ferromagnetic or three row-wise antiferromagnetic states[16,18] with three different $\mathbf{q}$ vectors. The row-wise state is triple degenerated up to the global rotation of magnetic moments; i.e., $W_{-}^{4-spin}=3$. If the coupling constant is positive ($J_{4-spin}>0$), a single ground state can be seen. This state is characterized by alternating ferromagneticlike and antiferromagneticlike rows [see Fig. 3(b)] and possess a fourfold degeneracy $W_{+}^{4-spin}=4$. In contrast to the spin structures induced by the biquadratic coupling, $W_{\pm}^{4-spin}$ does not depend on the sample size and, hence, the residual entropy of such a system is zero.

Thus, counterintuitive, the most dynamical, four-spin contribution to the exchange interaction leads to very stable magnetic configurations, while the pairwise biquadratic term results in a strong frustration of an itinerant system.

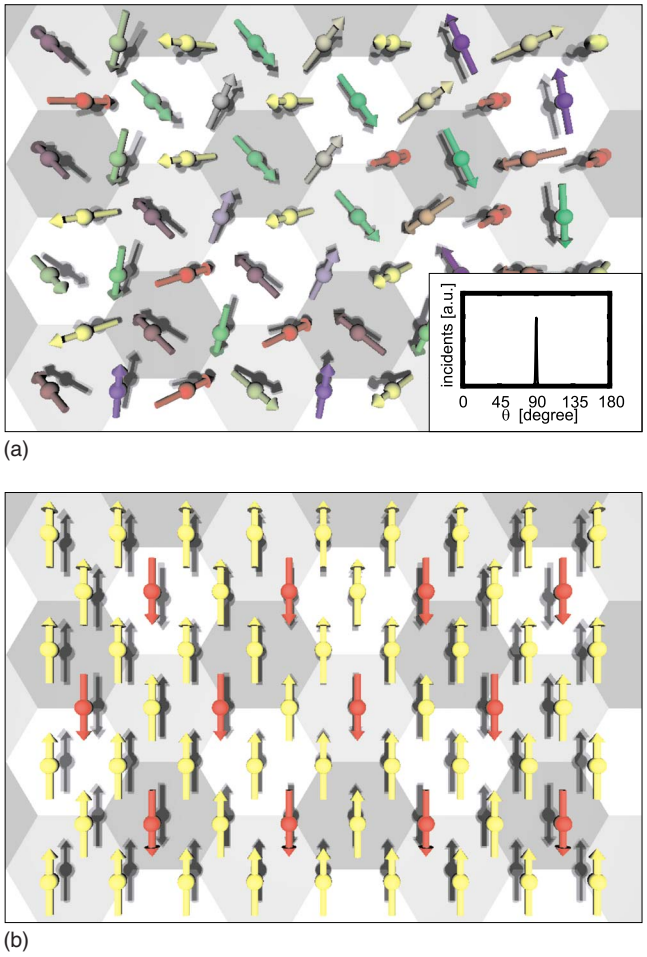

FIG. 3. (Color online) Top view of the ground states of a system with (a) pure biquadratic exchange interaction ($J_{bi}>0$) and (b) positive four-spin exchange coupling ($J_{4-spin}>0$). The inset shows a frequency distribution of angles between nearest-neighboring spins. Color scheme denotes the spatial orientation of the sublattices.

IV. MAGNETIC ORDERING IN TWO-DIMENSIONAL ITINERANT SYSTEMS: Mn/Cu(111) AND V/Ag(111)

It has been recently shown that monolayers of Mn and V deposited on a substrate with a hexagonal symmetry are ideal candidates for physical realizations of frustrated two-dimensional itinerant antiferromagnets.[9] Mn/Cu(111) and V/Ag(111) belong to the very few systems of this sort, which have been investigated from the first principles.[10] The ground state of Mn/Cu(111) is postulated to be a so-called $3q$ configuration (see Fig. 4),[2] which is a superposition of three spin spirals with different wave vectors q. The $3q$ symmetry is characterized by the tetrahedron angle $\theta=109.47°$ between nearest-neighboring spins. In the framework of the nearest-neighbor Heisenberg model without higher-order in-

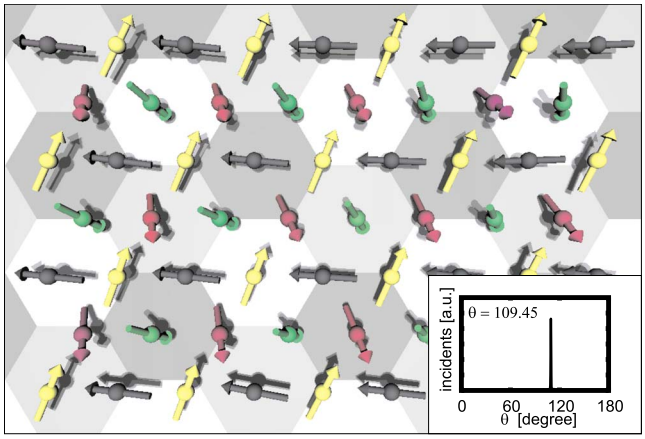

(a)

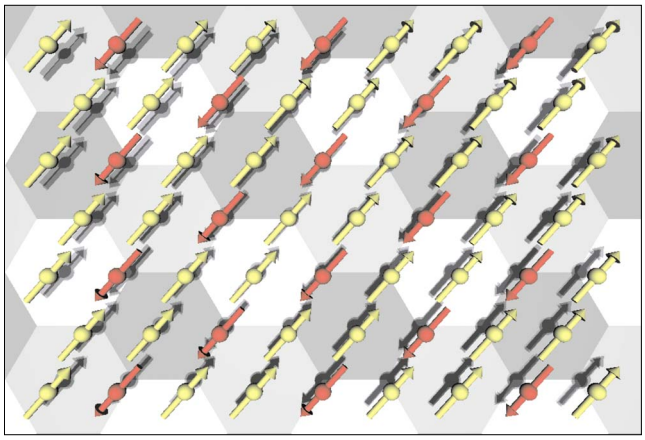

(b)

FIG. 4. (Color online) Top view of the ground state ($3q$ state) of a monolayer Mn on Cu(111) (a) and the ground state [collinear ferrimagnetic state (FI)] of a monolayer V on Ag(111) (b).

teractions, the $3q$ state and the row-wise antiferromagnetic configuration are degenerated. The higher-order terms choose the noncollinear $3q$ structure from the manifold of degenerated configurations.

For V/Ag(111), there is no unambiguous prediction of the ground state. Among five different possibilities investigated in Ref. 10, two configurations have almost identical energy. Those are a collinear structure that has been called a ferrimagnetic state (FI) (see Fig. 4) and the noncollinear Néel configuration (see Fig. 5). The striking feature of the FI structures is its uncompensated nature. The FI configuration has a net magnetization of $0.3\langle M_s\rangle$, where M_s is the saturation magnetization. The uncompensated antiferromagnetic structures are extremely important for possible exchange-bias applications.[19] Therefore, the understanding of the magnetic structuring in V/Ag(111) as well as in Mn/Cu(111) is of high interest for the basic knowledge of frustrated systems and for applications.

In case of strong degeneracy, like in V/Ag(111), often smaller energy contributions such as dipolar interactions, quantum or temperature fluctuations play a crucial role in the lifting of the degeneracy and ordering at low temperatures.[20–23] These energy contributions were not included in the first-principles calculations.[10] Another, related question which has not been addressed so far concerns the ordering phase transition at low temperatures. It is well known that according to the Mermin-Wagner theorem, no ordered phase can exist in an Heisenberg ferro- or antiferromagnet at finite temperature.[24] On the other hand, the frustration,[25–27] long-range,[28,29] or nonlinear[30–32] interactions as well as anisotropy[28,33–36] may induce an ordering phase transition in real systems. An exciting question is whether the higher-order exchange interactions belong to the class of factors stabilizing the magnetic ordering at finite temperatures.

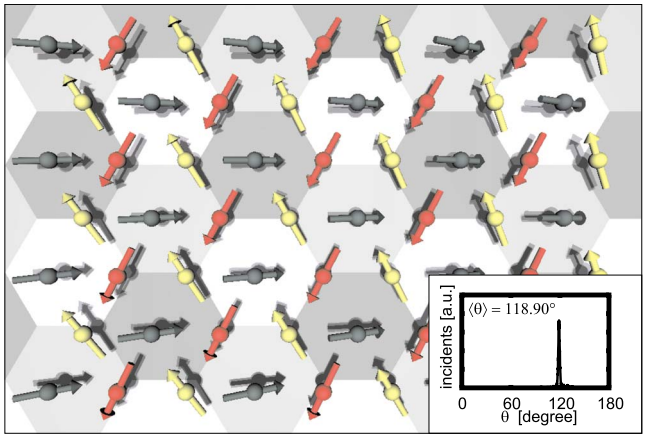

FIG. 5. (Color online) Top view of the Néel state which occurs below the ordering transition at $T=20$ K in V/Ag(111).

To answer the posed questions, we have studied the magnetic ordering and thermodynamic properties of Mn/Cu(111) and V/Ag(111) by means of Monte Carlo simulations. The material constants have been taken from the calculations.[10] For Mn on Cu(111) the Heisenberg nearest (J_1), next nearest (J_2) and next-next nearest (J_3) exchange interaction constants are $J_1=-31.2$ meV, $J_2=-13.9$ meV, and $J_3=-3.4$ meV. The biquadratic exchange constant and the four-spin interaction parameter are $J_{bi}=0.5$ meV and $J_{4-spin}=-2.6$ meV, respectively. The magnetic moment μ_s has a value of $\mu_s=3.05\mu_B$ and the lattice parameter a of Cu(111) is $a_{\mathrm{Cu(111)}}=3.604$ Å. This gives a value of the dipolar interaction $\omega=0.011$ meV, which is small compared to the exchange coupling. Test calculations have shown that the dipolar energy is lower than the critical thermal energy of the ordering phase transition. In the following, we neglect this interaction. The strength of the anisotropy D_z is assumed to be small.

In the case of V on Ag(111), following parameters have been used $J_1=-14.4$ meV, $J_2=9.9$ meV, $J_3=7.6$ meV, $J_{bi}=1.9$ meV, and $J_{4-spin}=0.1$ meV.

For both materials, we get stable ordered spin configurations for small but finite temperatures. Hence, it seems that the higher-order exchange contributions stabilize the magnetic ordering. In order to check this statement, we have performed calculations of the specific heat $C(T,L)$, the order parameters m, n, and the susceptibility $\chi(T,L)$ for different sample sizes L. The sublattice magnetization (root mean square)

$$m = \sqrt{\langle \mathbf{S}^2 \rangle}. \tag{4}$$

and the parameter n defined via the normalized difference between θ the angle between neighboring magnetic moments, and the mean value of θ in disordered state $\langle \theta_\infty \rangle = 90°$

$$n = \frac{|\langle \theta \rangle - \langle \theta_\infty \rangle|}{|\theta_0 - \langle \theta_\infty \rangle|}, \tag{5}$$

have been used as two independent order parameters. The angle θ_0 in Eq. (5) corresponds to θ of an ideal ground state and equals 0° or 180° for collinear, while 109.47° for the $3q$ configuration. Using $\beta=(kT)^{-1}$, $C(T,L)$ and $\chi(T,L)$ are deduced applying the fluctuation-dissipation theorem $C = \beta^2(\langle E^2 \rangle - \langle E \rangle^2)$ and $\chi = \beta \langle E \rangle (\langle m^2 \rangle - \langle m \rangle^2)$. Figures 6 and 7 show the thermodynamic characteristics for Mn/Cu(111) and V/Ag(111), respectively. Both systems show maxima of specific heat and susceptibility at the same temperature T_0 confirming the existence of a phase transition. A finite size scaling analysis showed that critical exponents are larger than those of the Ising universality class. However, this complex problem require additional investigations.

For Mn/Cu(111), the continuous ordering transition takes place at $T_0 \approx 50$ K (see Fig. 6). In accordance with Ref. 2, a $3q$ noncollinear configuration evolves below the critical temperature (Fig. 4). The V/Ag(111) shows more intriguing thermodynamic behavior. Instead of one single critical temperature, we find two distinct configurational phase transitions. The first one, at $T_0 \approx 130$ K, is driven by the formation of the ordered Néel state, as shown in Fig. 5. The second transition to collinear FI state happens at much lower temperature $T_1 \approx 20$ K as follows from the specific heat measurements of Fig. 7(a). The inset of Fig. 7(a) shows the corresponding energy kink in the same temperature range around the second phase transition. Very distinct features at the same temperature have also been found in the functions $\chi(L,T)$ and $n(L,T)$. Our calculations show that this phase transition appears for system sizes $L > 16$ and remains until $L \to \infty$. The total magnetization M of the system shows a jump from $M \approx 0$ (compensated Néel state) to finite values (FI state), which portends to a first order transition [see Fig. 7(b)].

Thus, our calculations demonstrate that the higher-order contributions to the exchange energy stabilize the low-temperature nontrivial ordering in itinerant magnets. In the following, we discuss an unpredicted double phase transition in V/Ag(111) and the role of individual energy contributions for the magnetic structuring.

Our calculations show that the internal energy of the Néel configuration lies approximately 1 meV higher than that of the ferrimagnetic structure (FI) for interaction parameters of V/Ag(111) [see Fig. 4(b)]. However, the number of available states for the Néel configuration is much larger than those of collinear FI configuration. Indeed, the Néel structure consists of three sublattices with mutual 120° orientation. If the orientation of one of the three sublattices is fixed, then

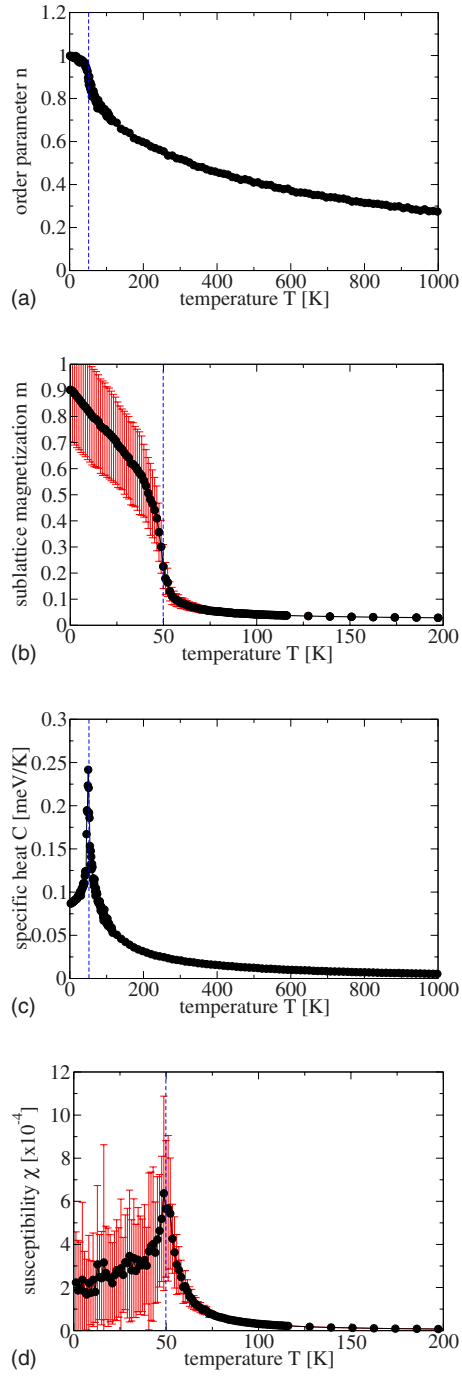

FIG. 6. (Color online) Thermodynamic characteristics found in MC calculations for Mn/Cu(111): (a) ordering parameter n, (b) sublattice magnetization m (averaged over 50 MC runs), (c) specific heat C, and (d) sublattice susceptibility χ (averaged over 50 MC runs).

two other subtilings may admit any orientation on a cone, whose generating line makes 120° with the orientation of the first sublattice. The total energy is independent of the azimuthal direction of the second and the third sublattice vectors; i.e., this particular Néel configuration is $2\pi\rho(\phi)$ times degenerated, where $\rho(\phi)$ is the azimuthal density of states.[16] The same is true for the two other sublattices. In total, $W_N = 8\pi^3\rho(\phi)^3$ degenerated states exist up to the global rota-

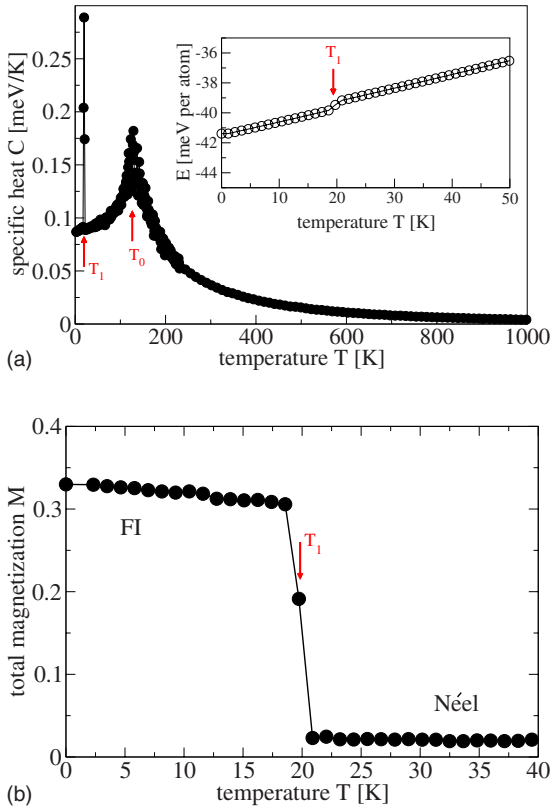

FIG. 7. (Color online) Temperature dependence of the specific heat (a) and total magnetization M (b) in V/Ag(111) for the sample size $L=128$: $T_0 \approx 130$ K marks the ordering temperature and $T_1 \approx 20$ K the structural transition temperature. The inset shows the corresponding energy in the range of the structural phase transition.

tion of the whole system. The FI configuration [see Fig. 4(b)] has only two collinear sublattices. Therefore, the FI state possesses only a threefold degeneracy $W_{FI}=3$ up to the global rotation. Hence, in contrast to the pure biquadratic ground state neither the Néel nor the FI configuration depends on the size of a lattice, i.e., the residual entropy is zero in both cases. However, the entropy of the Néel state S_N is for all sizes larger than that of the FI configuration S_{FI}.

The approaching to equilibrium is governed by the minimization of the free energy $F=E-TS$ with the internal energy E and the entropy $S=k \ln W$. The first higher temperature transition has an entropic character; i.e., $T(S_N-S_{FI})>(E_N-E_{FI})$ and therefore $F_N<F_{FI}$. For 120 K$>T>$20 K, a system spends the majority of time in one of the $8\pi^3\rho(\phi)^3$ Néel configurations (spin liquid). At $T \leqslant 20$ K, the TS contribution becomes lower than the energy difference $E_N-E_{FI}=1$ meV and the second phase transition governed by the internal energy appears. The system freezes in a FI state, which has zero residual entropy. From the considerations given above, the upper limit of the configurational entropy in V/Ag(111) can be estimated as $S=(E_N-E_{FI})/130\ \text{K}=7.69\times10^{-6}$ eV/K.

To clarify the role of higher-order energy contributions for the formation of ground states given in Fig. 4, the energies of characteristic configurations have been calculated with a stepwise neglecting of the four-spin and the biquadratic

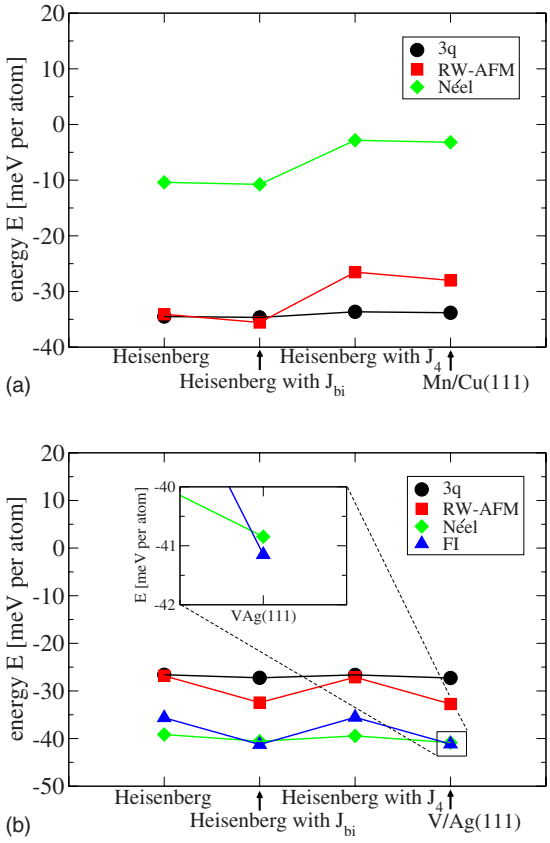

FIG. 8. (Color online) Internal energies of ideal magnetic configurations [circle, $3q$ state ($3q$); square, row-wise antiferromagnetic ordering (RW-AFM); diamond, Néel state; triangle up, collinear ferrimagnetic state (FI)]. The energies are calculated including Heisenberg exchange interaction only [up to third order, first sum in Eq. (1)], Heisenberg exchange with additional biquadratic exchange (first and second sum), Heisenberg exchange with additional four-spin interaction (first and fifth sum), and Heisenberg exchange with additional biquadratic exchange and four-spin interaction [all terms in Eq. (1)] in the case of (a) Mn/Cu(111) and (b) V/Ag(111).

couplings for Mn/Cu(111) [see Fig. 8(a)] and V/Ag(111) [see Fig. 8(b)]. As can be seen from Fig. 8(a), in the case of Mn/Cu(111), the RW-AFM is fully degenerated with the $3q$ state within the pure Heisenberg model. The addition of biquadratic exchange increases the total energy by a very small amount of 0.5 meV making the RW-AFM state slightly more favorable. However, the main role is played by the four-spin interaction which decreases the total energy by $J_{4\text{-}spin}=-2.6$ meV and by that means leaves up the degeneracy in favor of the $3q$ state. In the case of V/Ag(111), the biquadratic exchange ($J_{bi}=1.9$ meV) as well as the four-spin interaction ($J_{4\text{-}spin}=0.1$ meV) have a positive value. This means that the collinear structures become more favorable after adding the higher-order interactions.

V. SUMMARY

Magnetic ordering in itinerant antiferromagnetic monolayers with geometric frustration has been studied

theoretically for the examples of Mn on Cu(111) and V on Ag(111). For the appropriate description of the itinerant magnetism, exchange interactions beyond the Heisenberg model have been taken into account. We demonstrate that the ground states of both systems are quite different from those found in the framework of the traditional description within the Heisenberg model. We find that the higher-order exchange interactions stabilize the magnetic ordering and lead to configurational phase transitions at finite temperatures. A new, entropy driven phase transition is predicted for the system in V/Ag(111).

ACKNOWLEDGMENTS

The authors gratefully acknowledge the help of S. Krause processing some pictures and S. Heinze for helpful discussions. This work has been supported by the Deutsche Forschungsgemeinschaft in the framework of the project A11 of the SFB 668.

[1] D. Hobbs and J. Hafner, J. Phys.: Condens. Matter **12**, 7025 (2000).
[2] P. Kurz, G. Bihlmayer, K. Hirai, and S. Blügel, Phys. Rev. Lett. **86**, 1106 (2001).
[3] S. Heinze, P. Kurz, D. Wortmann, G. Bihlmayer, and S. Blügel, Appl. Phys. A **75**, 25 (2002).
[4] G. Bihlmayer, P. Ferriani, S. Baud, M. Ležaić, S. Heinze, and S. Bügel, in *NIC Symposium 2006*, NIC Series Vol. 32, edited by G. Münster, D. Wolf, and M. Kremer (John von Neumann Institute for Computing, Jülich, 2006).
[5] G. M. Stocks, M. Eisenbach, B. Újfalussy, B. Lazarovits, L. Szunyogh, and P. Weinberger, Prog. Mater. Sci. **52**, 371 (2007).
[6] E. Y. Vedmedenko, U. Grimm, and R. Wiesendanger, Phys. Rev. Lett. **93**, 076407 (2004).
[7] A. H. MacDonald, S. M. Girvin, and D. Yoshioka, Phys. Rev. B **37**, 9753 (1988).
[8] D. Wortmann, P. Kurz, S. Heinze, K. Hirai, G. Bihlmayer, and S. Blügel, J. Magn. Magn. Mater. **240**, 57 (2001).
[9] P. Kurz, G. Bihlmayer, S. Blügel, K. Hirai, and T. Asada, Phys. Rev. B **63**, 096401 (2001).
[10] P. Kurz, Ph. D. thesis, RWTH Aachen, 2000.
[11] W. H. Press, B. P. Flannery, S. A. Teukolsky, and W. T. Vetterling, *Numerical Recipes* (Cambridge University Press, Cambridge, 1990).
[12] D. Hinzke and U. Nowak, J. Magn. Magn. Mater. **221**, 365 (2000).
[13] U. Nowak, R. W. Chantrell, and E. C. Kennedy, Phys. Rev. Lett. **84**, 163 (2000).
[14] D. Hinzke and U. Nowak, Phys. Rev. B **61**, 6734 (2000).
[15] U. Nowak, in *Annual Reviews of Computational Physics IX*, edited by D. Stauffer (World Scientific, Singapore, 2001), p. 105.
[16] E. Y. Vedmedenko, *Competing Interactions and Pattern Formation in Nanoworld* (Wiley, Weinheim, 2007).
[17] G. H. Wannier, Phys. Rev. **79**, 357 (1950).
[18] P. Kurz, F. Förster, L. Nordström, G. Bihlmayer, and S. Blügel, Phys. Rev. B **69**, 024415 (2004).
[19] M. Bode, E. Y. Vedmedenko, K. von Bergmann, S. Heinze, A. Kubetzka, and R. Wiesendanger, Nat. Mater. **5**, 477 (2006).
[20] B. C. denHertog and M. J. P. Gingras, Phys. Rev. Lett. **84**, 3430 (2000).
[21] S. E. Palmer and J. T. Chalker, Phys. Rev. B **62**, 488 (2000).
[22] S. Sachdev, Phys. Rev. B **45**, 12377 (1992).
[23] E. Y. Vedmedenko, Phys. Status Solidi B **244**, 1133 (2007).
[24] N. D. Mermin and H. Wagner, Phys. Rev. Lett. **17**, 1133 (1966).
[25] H. Kawamura, J. Appl. Phys. **61**, 3590 (1987).
[26] C. L. Henley, Phys. Rev. Lett. **62**, 2056 (1989).
[27] J. E. Greedan, J. Mater. Chem. **11**, 37 (2001).
[28] P. Bruno, Phys. Rev. B **43**, 6015 (1991).
[29] J. Sasaki and F. Matsubara, J. Phys. Soc. Jpn. **67**, 1134 (1998).
[30] H. W. J. Blöte, W. Guo, and H. J. Hilhorst, Phys. Rev. Lett. **88**, 047203 (2002).
[31] S. Caracciolo and A. Pelissetto, Phys. Rev. E **66**, 016120 (2002).
[32] A. C. D. van Enter and S. B. Shlosman, Phys. Rev. Lett. **89**, 285702 (2002).
[33] J. M. Kosterlitz and D. J. Thouless, J. Phys. C **6**, 1189 (1973).
[34] L. Capriotti, R. Vaia, A. Cuccoli, and V. Tognetti, Phys. Rev. B **58**, 273 (1998).
[35] W. Stephan and B. W. Southern, Phys. Rev. B **61**, 11514 (2000).
[36] U. Krey, J. Magn. Magn. Mater. **268**, 277 (2004).